PCCP

ROYAL SOCIETY OF CHEMISTRY

COMMUNICATION

View Article Online
View Journal

Cite this: DOI: 10.1039/d3cp00142c

Received 10th January 2023,
Accepted 28th February 2023

DOI: 10.1039/d3cp00142c

rsc.li/pccp

Origin and remedy for HSQC artifacts in proton-detected INADEQUATE spectra†

R. Thomas Williamson *[a] and Ole W. Sørensen *[b]

NMR pulse sequences visualizing $^{1}J_{CC}$ and $^{n}J_{CC}$ bond connectivity *via* an intermediate state of ^{13}C–^{13}C double-quantum coherence and ^{1}H detection are an indispensable tool to solve small-molecule structures at the natural abundance level of ^{13}C. A longstanding issue with these experiments set up to display 2D spectra with single-quantum frequencies is that in addition to the ^{1}H–^{13}C–^{13}C correlations of interest, appearance of HSQC-type artifacts can complicate analysis and obscure J_{CC} connectivities. The origin of these artifacts is described and remedies for their suppression are introduced. They include refocusing of $^{1}J_{CH}$ couplings prior to creation of ^{13}C–^{13}C double-quantum coherence, which is known to enhance sensitivity by reducing loss into zero-quantum coherence for pairs of two protonated ^{13}C.

When conventional homonuclear and heteronuclear NMR experiments relying on molecules with a single ^{13}C spin fail to provide an unambiguous structural solution in small-molecule NMR, the experiments of last resort typically rely on molecules with two mutually coupled ^{13}C spins.[1] Besides the rare natural abundance of two coupled ^{13}C spins (0.012%), the desired signals of ^{1}H–^{13}C–^{13}C moieties can easily be obscured by a background of signals two and four orders of magnitude larger from ^{1}H–^{13}C–^{12}C and ^{1}H–^{12}C–^{12}C isotopomers, respectively.

Fortunately, application of pulsed field gradients effecting double-quantum (DQ) filtration and phase cycles selecting coherence transfer pathways involving ^{13}C–^{13}C DQ coherence yield spectra almost exclusively from the doubly ^{13}C-labeled molecules suppressing the much larger undesired signals.[2–8] This category of techniques was introduced as proton-detected INADEQUATE (PDI) experiments with reference to the corresponding experiment with ^{13}C detection.[9]

The most popular PDI pulse sequences currently in use are based on the 1996 reports by Reif and coworkers.[6,7] This family of experiments given the truncated acronym of ADEQUATE was comprised of 1,1-, 1,*n*-, *n*,1-, and *n*,*n*-ADEQUATE. A report published in the same time period demonstrated how refocusing of $^{1}J_{CH}$ couplings prior to creation of ^{13}C–^{13}C DQ-coherence using INEPT or DEPT can enhance sensitivity and provided optimum settings for the different pairs of ^{13}C multiplicities.[8]

Historically, NMR spectroscopists prefer the more familiar ^{13}C single-quantum (SQ) over DQ frequencies in the indirect dimension which led Reif *et al.* to design a pulse sequence with a module that results in one of the ^{13}C SQ frequencies being subtracted from the ^{13}C–^{13}C DQ frequency, thus leading to correlations at the ^{13}C frequency of the complementary spin in the pair.[6] When that ^{13}C spin is remote relative to the detected ^{1}H spin, the peak represents a correlation of interest. On the other hand, if the ^{13}C spin is attached to the detected ^{1}H spin, the response represents an undesired HSQC-type correlation.

These contributions were apparently not expected to make it through to detection because of the antiphase character with respect to the remote proton prior to back-transfer from ^{13}C to ^{1}H magnetization and ^{13}C decoupling during the ^{1}H-detected FID. However, whilst that holds true for a simple INEPT back-transfer, it generally does not for the usual more elaborate coherence-order-selective (COS) back-transfer.

Importantly, both the PDI correlations of interest and the undesired artifacts originate from molecules with two coupled ^{13}C spins. Neither gradients nor phase cycles can suppress the artifacts because they pass through the same window of coherence transfer pathways for the desired signals.

A recent paper[10] has observed that refocusing of $^{1}J_{CH}$ antiphase structure prior to DQ creation yields some suppression of HSQC artifacts and that these artifacts are largely absent for correlations based on long-range J_{CC} couplings. The current Communication fully accounts for the origin and features of the HSQC artifacts and presents a remedy for their enhanced suppression.

In the family of PDI-1 experiments outlined in Fig. 1, there are two evolution periods. (The "1" in PDI-1 indicates

[a] *Department of Chemistry & Biochemistry, University of North Carolina Wilmington, Wilmington, North Carolina 28409, USA. E-mail: williamsonr@uncw.edu*

[b] *Copenhagen, Denmark. E-mail: sorensen.ole.w@gmail.com*

† Electronic supplementary information (ESI) available. See DOI: https://doi.org/10.1039/d3cp00142c

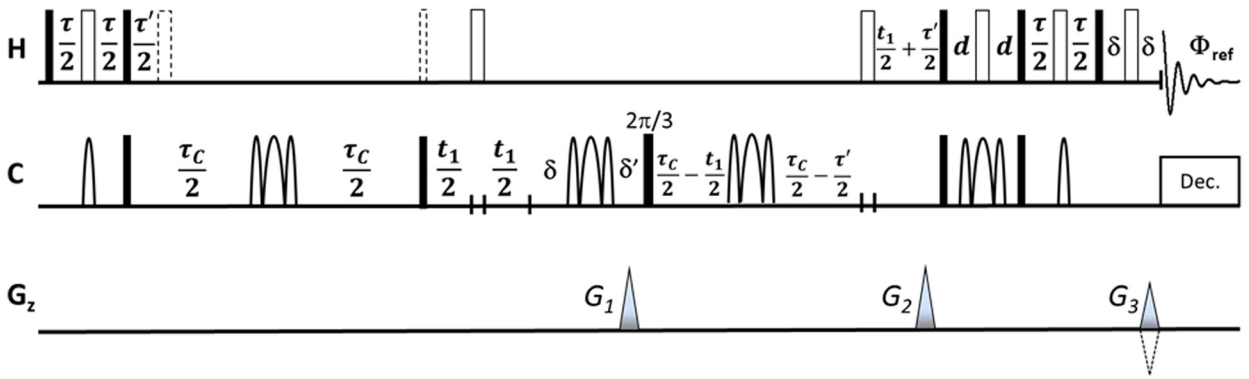

Fig. 1 PDI-1 NMR pulse sequences in condensed form referred to as (A), (B) and (C) for the three versions: (A) The one described by Reif *et al.* where the dashed pulses are excluded and $\tau' = 0$. (B) Refocused version with the dashed π pulse and the τ' delays included leading to some suppression of HSQC-type correlations. (C) Further refined pulse sequence for suppression of HSQC-type artifacts with both dashed pulses and the τ' delays included. $\tau = 0.5/({}^1J_{CH})$, $\tau_C \approx 0.5(2k+1)/({}^1J_{CC})$ where k is an integer, and the delay d set according to ^{13}C multiplicity but in practice most often $d = \tau/2$ and τ set according to the average ${}^1J_{CH}$ in the methine groups. Optimization for methylene or methyl groups requires shorter τ' delays.[8] The setting $\tau' = \tau$ in (B) and (C) results in double sensitivity for methine–methine pairs. Phase cycles and gradient ratios can be as described in ref. 6. The three versions of PDI–1 are outlined separately in Fig. S1 (ESI†).

polarization transfer from ^{1}H to ^{13}C *via* ${}^1J_{CH}$.) In the first, DQ coherence (at + or − the sum of the chemical shifts of the two ^{13}C spins involved) is present, and in the second, SQ coherence of opposite sign for one of the ^{13}C spins is selected. The chemical shift of the active spin during the second evolution period is the one subtracted from the DQ frequency. What remains is the chemical shift frequency of the complementary ^{13}C spin in the ^{13}C–^{13}C pair. The subsequent back-transfer conveys magnetization of the active ^{13}C spin to its attached proton(s), from where the magnetization originated, for detection. The result is a 2D spectrum in the familiar format of ^{13}C and ^{1}H SQ frequencies in the F_1 and F_2 dimensions, respectively, and from the viewpoint of the protons showing correlation peaks to carbons two or more bonds away. Unfortunately, there is also a route in the back-transfer from the complementary ^{13}C spin to the attached proton(s) of the ^{13}C partner spin made possible by the heteronuclear COS module that thus has the side effect of allowing undesired HSQC artifact contributions to pass through.

Another peculiarity observed in PDI-1 spectra over the years is that the protons with a resolved J_{HH}, as *e.g.* a vicinal coupling in neighboring ^{13}C–^{13}C methine pairs, appear with an enhanced doublet splitting in the PDI peaks compared to a regular HSQC spectrum whilst the corresponding HSQC artifacts show the opposite effect of a ''blurred'' or unresolved doublet. These anomalies also arise from the route opened for HSQC artifacts by the COS back-transfer module.

A product operator analysis[11–13] of the antiecho pathway starting at the $2\pi/3$ pulse in the pulse sequence of Fig. 1A for a methine–methine spin system (I_1S_1–I_2S_2 with I and S representing ^{1}H and ^{13}C, respectively) can be found in ESI.† The result detected on the ^{1}H spin I_1 applicable for both echo and antiecho can be expressed as the following.

PDI peaks:

$$\left\{\frac{i}{2}I_1^- \sin(\pi J_{CC}\tau_C) + \frac{1}{2}2I_1^- I_{2z}\cos(\pi J_{CC}\tau_C)\right\}(1+\cos(\pi J_{CC}2d)) \quad (1)$$

HSQC peaks:

$$\left\{-\frac{i}{2}I_1^- \cos(\pi J_{CC}\tau_C) + \frac{1}{2}2I_1^- I_{2z}\sin(\pi J_{CC}\tau_C)\right\}\sin(\pi J_{CC}2d) \quad (2)$$

or split up in the two ^{1}H doublet components:

$$\{I_1^- I_2^\alpha e^{i\pi J_{CC}\tau_C} - I_1^- I_2^\beta e^{-i\pi J_{CC}\tau_C}\}(1+\cos(\pi J_{CC}2d)) \quad (1')$$

$$-i\{I_1^- I_2^\alpha e^{i\pi J_{CC}\tau_C} + I_1^- I_2^\beta e^{-i\pi J_{CC}\tau_C}\}\sin(\pi J_{CC}2d) \quad (2')$$

In product operator terminology, I_1^- represents inphase doublet magnetization and $2I_1^- I_{2z}$ represents the doublet magnetization in antiphase with respect to the coupling to the I_2 spin. $I_1^- I_2^\alpha$ and $I_1^- I_2^\beta$ represent magnetization of the I_1 doublet component with the I_2 spin in the α and β state, respectively.

The product operator analysis in ESI† provides the pertinent full story, but key features can be observed in the expressions above.

• Even when no J_{CC} refocusing takes place in the τ_C delay (*i.e.* $J_{CC}\tau_C = k\cdot\pi$, $k = 0, 1, 2, \ldots$) after the $2\pi/3$ pulse and the dominant inphase term, I_1^-, vanishes for the PDI peaks there will be a full intensity PDI peak arising through the alternate coherence transfer route leading to the antiphase term $2I_1^- I_{2z}$. For such a setting the HSQC peaks come through as inphase magnetization.

• The factor $\sin(\pi J_{CC}2d)$ for the HSQC artifacts is indicative of a refocusing of a product operator antiphase with respect to J_{CC} during the delay $2d$. Since that delay is tuned according to ${}^1J_{CH}$ it follows that HSQC artifacts are a phenomenon associated exclusively with neighboring ^{13}C spins sharing a ${}^1J_{CC}$. Contributions from different neighboring ^{13}C spins co-add in the spectrum.

• The factor i on terms in the expressions indicates a $\pi/2$ phase shift relative to terms without that factor.

• For a perfectly matched delay $\tau_C = 0.5/J_{CC}$ the PDI doublets are in-phase and the HSQC artifact doublets are antiphase and in dispersion if the PDI doublets are phased to absorption.

• For a mismatched delay τ_C, both the PDI and the HSQC artifact doublets are a superposition of an inphase term and a

"triplet" (arising from the dispersive antiphase doublet structure) with inverted outer lines. If the central part of the "triplet" points in opposite direction to the in-phase doublet, it causes a dip in the middle of the doublet that appears with enhanced resolution. On the other hand, if the central part of the "triplet" points in the same direction as the in-phase doublet, it fills the space between the two doublet components and thus blurs the splitting.

- For methine–quaternary ^{13}C–^{13}C pairs, the antiphase product operator in expression (1) is absent, so there is no HSQC artifact in such spin systems in case of a perfectly matched delay $\tau_C = 0.5/J_{CC}$.
- A setting of $\tau_C = k/J_{CC}$, $k = 0, 1, 2, \ldots$, in the second τ_C delay (keeping $\tau_C = 0.5/J_{CC}$ in the first) will suppress all PDI peaks without a resolved J_{HH} between the protons attached to the two ^{13}C spins and retain full intensity HSQC peaks.

Below is shown a pictorial representation of expressions (1) and (2) where the term $\frac{i}{2}I_1^-$ by proper phase correction is a positive doublet in absorption whilst $\frac{1}{2}2I_1^-I_{2z}$ is an antiphase doublet in dispersion. Such an antiphase doublet in dispersion looks like a "triplet" with two negative outer lines and a positive central component resulting from overlap of the two oppositely oriented dispersive lineshapes. Depending on the size of J_{HH}, the central component of these "triplets" can show a splitting.

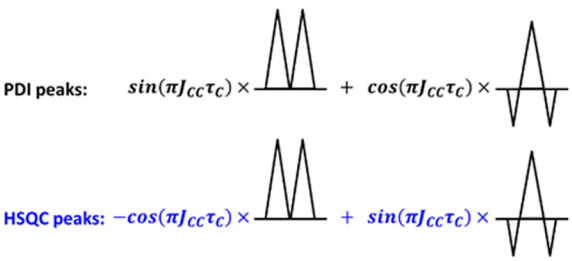

The features of expressions (1) and (2) are demonstrated in Fig. 2 using the C5H5–C6H6 spin system in hymecromone. The peakshapes and phases of the HSQC and PDI responses are in accordance with the product operator analysis and scheme above for the four J_{CC} evolution angles chosen in Fig. 2A–D, though minor strong coupling distortions are visible.

The product operator analysis describes how the HSQC artifacts arise and with that insight it is possible to design remedies to suppress them. For example, for the antiecho part originating from I_1 magnetization, there is a DQ product operator $4I_{1z}S_1^+S_2^+$ right before the $2\pi/3$ pulse in the pulse sequence by which that product operator is partly transferred to $4I_{1z}S_1^-S_{2z}$ and $4I_{1z}S_{1z}S_2^-$. Afterwards the π^C pulse in the τ_C delay inverts the sign of these SQ coherences, *i.e.* yielding $4I_{1z}S_1^+S_{2z}$ and $4I_{1z}S_{1z}S_2^+$, and most importantly the I_{1z} operator is maintained throughout the τ_C delay due to heteronuclear decoupling by the π^H pulse in the delay. As is evident in the product operator analysis, the I_{1z} operator is essential for production of HSQC artifacts. The first step is a coherence

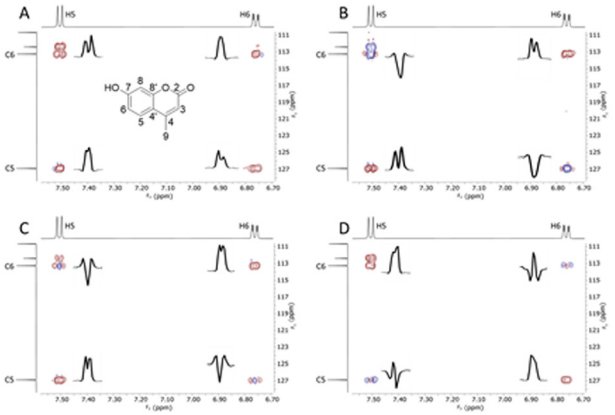

Fig. 2 Results of the PDI-1 pulse sequence in Fig. 1A with data acquired on a 100 mg sample of hymecromone dissolved in 750 μL DMSO-d_6 using a 500 MHz Bruker Neo NMR spectrometer equipped with a 5 mm Prodigy TCI Cryoprobe. The delay $\tau = \tau'$ was set for J_{CH} = 160 Hz and the first τ_c delay for J_{CC} = 60 Hz. The second τ_c delay was set to accomplish: (A) $\pi J_{CC}\tau_C = \frac{\pi}{2}$, (B) $\pi J_{CC}\tau_C = \pi$, (C) $\pi J_{CC}\tau_C = \frac{3\pi}{4}$, and (D) $\pi J_{CC}\tau_C = \frac{5\pi}{4}$. The acquisition time with GARP decoupling was 246 ms and recorded 3k data points. 48 scans were acquired for each of the 180t_1 increments. Data were processed as a 4k × 1k matrix with a $\pi/2$ shifted sine squared apodization applied in both dimensions and linear prediction to 384 data points in t_1 before Fourier transformation.

transfer from the S_2 magnetization $4I_{1z}S_{1z}S_2^+$ to S_1 by the $(\pi/2)^C$ pulse at the end of the τ_C delay. All in all, the resulting relevant product operator is $4I_{1y}S_{1y}S_{2z}$ and it is the refocusing of the S_1–S_2 antiphase character to $2I_{1y}S_{1x}$ during the $2d$ delays that gives rise to the factor $\sin(\pi J_{CC}2d)$ in expressions (2) and (2′). Eventually, this product operator makes it through to become I_1 inphase magnetization labeled with the S_1 chemical shift from the evolution periods and thus gives rise to an I_1–S_1 HSQC artifact. The antiphase HSQC artifact term arises *via* another route but common to both contributions is that they require the I_{1z} operator at the end of the τ_C delay. The desired PDI peaks also need that operator for back-transfer, but the key point is that in those terms it is associated with its attached S spin (*i.e.* I_{1z} associated with S_1^+). In contrast, for the HSQC artifacts it is associated with the remote S spin (*i.e.* I_{1z} associated with S_2^+), or in other words, the S_2 spin is associated with a "foreign" I_z operator. Thus, a remedy for HSQC artifacts is to avoid product operators with "foreign" I_z operators in the second τ_C delay.

This goal can be accomplished by having no I_z operators immediately after the $2\pi/3$ ^{13}C pulse. That in turn requires that the heteronuclear antiphase structure after the initial INEPT polarization transfer is refocused prior to DQ excitation. This scenario would yield product operators $2S_1^-S_{2z}$ and $2S_{1z}S_2^-$ right after the $2\pi/3$ ^{13}C pulse rather than $4I_{1z}S_1^-S_{2z}$ and $4I_{1z}S_{1z}S_2^-$ as described above for the pulse sequence in Fig. 1A. The modification necessary for this is the dashed π^H pulse and the τ' delays in Fig. 1, *i.e.* the pulse sequence represented by Fig. 1B.

To prepare for the back-transfer, the product operators $2S_1^+S_{2z}$ and $2S_{1z}S_2^+$ are made antiphase with respect to $^1J_{CH}$ through the addition of the second τ' delay to become $4I_{1z}S_1^+S_{2z}$ and

$4S_{1z}I_{2z}S_2^+$ which both contain a "home" I_z operator (an I_z operator with the same house number as the transverse S operator, *i.e.* a ^1J-connected I–S pair) that does not produce HSQC artifacts. Such refocused pulse sequences were in fact included in a DEPT implementation in the paper by Meissner *et al.*,[8] but at that time there was no awareness of HSQC artifacts that are not obvious in spectra displaying DQ frequencies in the F_1 dimension.

Complete elimination of "foreign" I_z operators in the second τ_C delay hinges for methine groups on a perfect match of $\tau' = 0.5/^1J_{CH}$ which generally is not possible since the J coupling constants in most molecules vary over a certain range. Any mismatch of τ' will leave some "foreign" I_z operators and thus call for an additional remedy to eliminate them. That remedy is a $(\pi/2)^H$ purging pulse[11] placed at the point of DQ excitation as represented by the dashed $(\pi/2)^H$ pulse in Fig. 1, *i.e.* the pulse sequence in Fig. 1C. The need for such a purging pulse is particularly pronounced in the presence of methylene and methyl groups because of incomplete refocusing. No compromise setting of τ' exists that can refocus the heteronuclear couplings for all multiplicities with a simple spin echo. Methylene and methyl groups require a τ' delay shorter than $0.5/^1J_{CH}$.

The $^1J_{CH}$ refocusing in the first and the defocusing in the second τ_C delay follow the intensity function for refocusing in INEPT.[11,14] More complete intensity expressions can be found in ref. 8.

Fig. 3 represents an application to hymecromone with PDI-1 spectra showing all the expected ^1H–^{13}C two-bond correlations resulting from the two-step polarization transfer process through two one-bond couplings. The first step transfers polarization from a proton to its attached carbon *via* $^1J_{CH}$ and the second step passes the polarization on to the ^{13}C neighbors *via* $^1J_{CC}$. Low-intensity peaks are due to a little polarization transfer between carbons separated by more than one chemical bond *via* longer-range J_{CC} couplings.

The simplest HSQC artifact remedy in the PDI-1 pulse sequence in Fig. 1B is quite effective in suppressing the artifacts, and possibly adequate in many applications. This is shown in Fig. 3B using the best compromise delay settings for hymecromone. In Fig. 3C it is shown how the additional "foreign I_z operator removal tool" in the form of the purging pulse in the pulse sequence in Fig. 1C almost fully purges the remaining HSQC artifacts on H3 and H8 whereas the suppression on H5 and H6 already is so high that little is gained by addition of the purging pulse. Pertinent F_2 sections can be found in Fig. S2 (ESI†). The ratio of desired peaks to artifacts for methine–methine pairs gains on two fronts, firstly through the signal being doubled compared to the reference experiment and secondly through the HSQC artifacts being suppressed. For methine–quaternary pairs the sensitivity is largely unaffected by the HSQC artifact suppression tools.

In ESI,† Fig. S3 shows F_2 sections through the H6–C5 methine–methine PDI peak and three methine–quaternary correlations. They illustrate for methine–methine pairs the about double sensitivity using the HSQC artifact-suppression PDI-1 versions in Fig. 1B and C in comparison to the version in Fig. 1A. Such a gain cannot be accomplished in

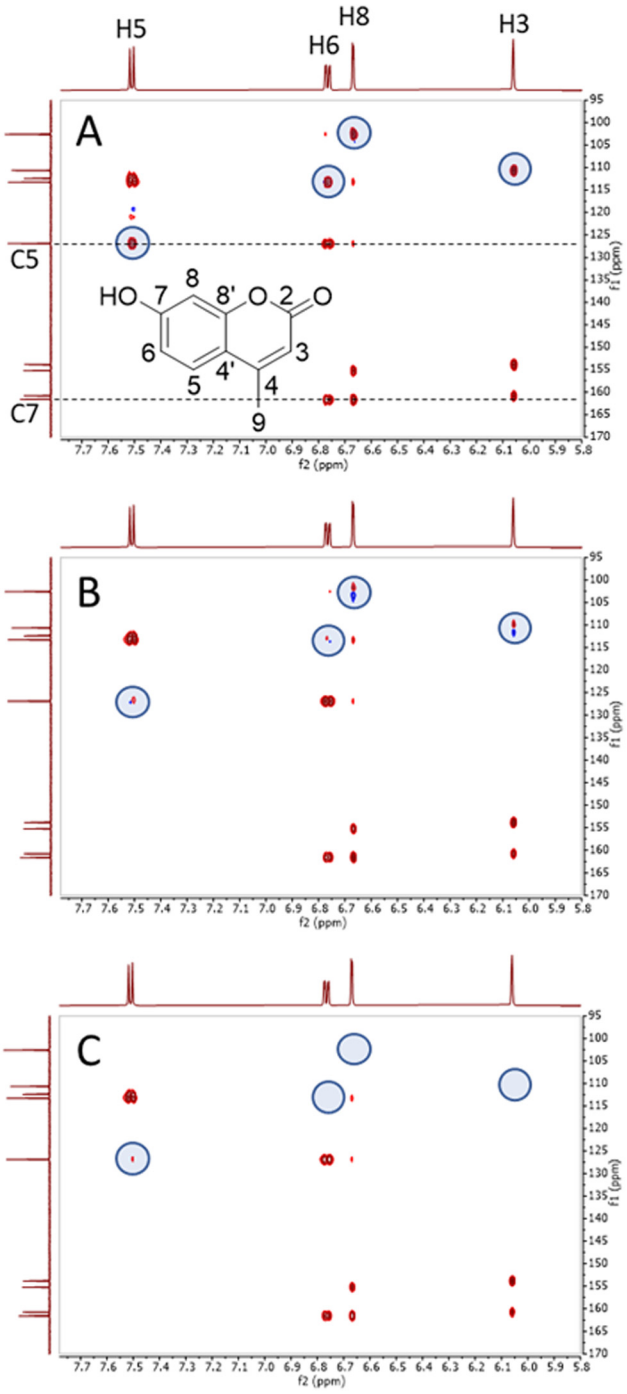

Fig. 3 Results of the pulse sequences depicted in Fig. 1 with (A–C) in that figure corresponding to (A–C) in this figure. Data were acquired on a 100 mg sample of hymecromone dissolved in 750 μL DMSO-d_6 using a 600 MHz Bruker AVIII NMR spectrometer with a 5 mm room temperature TXI probe. Shaded circles are put around HSQC responses, sections through which are shown in Fig. S2 (ESI†). The dashed lines indicate the locations of F_2 sections for C5 and C7 shown in Fig. S3 (ESI†). The delays $\tau = \tau'$ were set for J_{CH} = 160 Hz and τ_c for J_{CC} = 55 Hz. The acquisition time with GARP decoupling was 213 ms and recorded 3k data points. 80 scans were acquired for each of the 128t_1 increments. Data were processed as a 4k × 1k matrix with a π/2 shifted sine squared apodization applied in both dimensions and linear prediction to 256 data points in t_1 before Fourier transformation.

methine–quaternary systems because the quaternary carbons do not contribute magnetization into the DQ coherence, but fortunately the HSQC artifact-suppression additions to the pulse sequence do not significantly compromise the sensitivity either and HSQC artifact suppression is effective for those spin systems too.

The pulse sequence proposed by Sakas and Uhrin[10] corresponds to the PDI-1 version in Fig. 1B, because the applied WALTZ multipulse decoupling sequence does not cause randomization of ^{1}H spin operators.[15] In their pulse sequence it is an option to place a $(\pi/2)^{H}$ purging pulse simultaneous with the 120° (^{13}C) pulse.

In summary, we have described the origin of the ubiquitous HSQC artifacts in proton-detected INADEQUATE spectra laid out for 2D NMR data with ^{13}C single-quantum frequencies in the F_1 dimension and introduced remedies for their suppression. The simplest solution consists of refocusing $^{1}J_{CH}$ couplings prior to creation of ^{13}C–^{13}C DQ coherence, which might well provide an acceptable suppression level for many applications. Otherwise, a $(\pi/2)^{H}$ purging pulse can be added simultaneously with ^{13}C double-quantum excitation. Finally, a product operator analysis also showed the origin of the peculiarity of desired PDI peaks showing a well resolved homonuclear J splitting whilst HSQC artifacts on the same proton show an ill-resolved multiplet. These effects as well as the HSQC artifacts arise through a pathway opened by the COS back-transfer module.

Conflicts of interest

There are no conflicts to declare.

Acknowledgements

Support of NSF grant # 0821552 and 2116395 for purchase of the NMR spectrometers utilized in this work is acknowledged. Further funding was provided by the Yousry and Linda Sayed Endowment and Clemens Anklin (Bruker Biospin®) is thanked for helpful pulse programming suggestions.

Notes and references

1 (*a*) G. E. Martin, M. Reibarkh, A. V. Buevich, K. A. Blinov and R. T. Williamson, Development of 1,n-ADEQUATE and Modified Variants and their Application to Structure Elucidation and Spectral Assignment Problems, *eMagRes*, 2014, **3**, 215–234, DOI: **10.1002/9780470034590.emrstm1370**; (*b*) J. Saurí and G. E. Martin, NMR Experiments Applicable to the Elucidation and Characterization of Alkaloid Structures – Part II Advanced Techniques for the Identification of Adjacent Carbons Using H2BC, 1,1-ADEQUATE and Variants, in *Modern NMR Approaches to the Structure Elucidation of Natural Products*, ed. A. Williams, G. Martin and D. Rovnyak, RSC, London, 2016, vol. 2, pp. 358–402; (*c*) J. Saurí, I. E. Ndukwe, M. Reibarkh, Y. Liu, R. T. Williamson and G. E. Martin, New Variants of the ADEQUATE Experiments, *Ann. Rep. NMR Spectrosc.*, 2019, **98**, 1–56, DOI: **10.1016/bs.arnmr.2019.04.001**; (*d*) G. E. Martin, Using 1,1- and 1,n-ADEQUATE 2D NMR Data in Structure Elucidation Protocols, in *Annual Reports on NMR Spectroscopy*, ed. G. A. Webb, Elsevier, London, 2011, vol. 74, pp. 215–291.
2 P. J. Keller and K. E. Vogele, *J. Magn. Reson.*, 1986, **68**, 389–392.
3 Y. Q. Gosser, K. P. Howard and J. H. Prestegaard, *J. Magn. Reson., Ser. B*, 1993, **101**, 126–133.
4 J. Chung, J. R. Tolman, K. P. Howard and J. H. Prestegaard, *J. Magn. Reson., Ser. B*, 1993, **102**, 137–147.
5 J. Weigelt and G. Otting, *J. Magn. Reson., Ser. A*, 1995, **113**, 128–130.
6 B. Reif, M. Köck, W. Fenical and C. Griesinger, *Tetrahedron Lett.*, 1996, **37**, 363–366.
7 B. Reif, M. Köck, R. Kerssebaum, H. Kang, W. Fenical and C. Griesinger, *J. Magn. Reson., Ser. A*, 1996, **118**, 282–285.
8 A. Meisner, D. Moskau, N. C. Nielsen and O. W. Sørensen, *J. Magn. Reson.*, 1997, **236**, 245–249.
9 A. Bax, R. Freeman and T. A. Frenkiel, *J. Am. Chem. Soc.*, 1981, **103**, 2102–2104.
10 J. Sakas and D. Uhrin, *Chem. Commun.*, 2022, **58**, 13011–13014.
11 O. W. Sørensen and R. R. Ernst, *J. Magn. Reson.*, 1983, **51**, 477–489.
12 O. W. Sørensen, G. W. Eich, M. H. Levitt, G. Bodenhausen and R. R. Ernst, *Prog. NMR Spectrosc.*, 1983, **16**, 163–192.
13 O. W. Sørensen, *Prog. NMR Spectrosc.*, 1989, **21**, 503–569.
14 D. P. Burum and R. R. Ernst, *J. Magn. Reson.*, 1980, **39**, 163–168.
15 M. H. Levitt, G. Bodenhausen and R. R. Ernst, *J. Magn. Reson.*, 1983, **53**, 443–461.